Lithography

***Shinji Okazaki**, EUV Lithography Laboratory, ASET Atsugi Research Center, Japan*

***Jürgen Moers**, Department ISG, Research Center Jülich, Germany*

Contents

1 Survey 223

2 Optical Lithography 224
2.1 Illumination Methods and Resolution Limits 224
Resolution Enhancement 226
2.2 Exposure Wavelength and Light Sources 228
2.3 Mask Materials and Optical System 230
2.3.1 Set-up of the Optical Path 230
2.3.2 Reflection optics for short wavelengths 232

3 Extreme Ultraviolet Lithography 232

4 X-Ray Lithography 234

5 Electron Beam Lithography 234
5.1 Electron Beam Direct Write 235
5.2 SCALPEL 236

6 Ion Beam Lithography 237
6.1 Focused Ion Beam 237
6.2 Ion Projection Lithography 238

7 Photoresist 239

8 Alignment of Several Mask Layers 241

9 Nanoimprint Lithography 242

10 Conclusions 244

9

Lithography

1 Survey

Greek λιθοσ ´a stone´ and γραφειν ´to write´, the art of printing from stone is one of the most important of the graphic arts ...[1]

This short explanation found in an encyclopaedia is followed by several pages describing the different methods of this art. This explanation is right, but does not cover the meaning which is the topic of this chapter. Here *lithography* addresses the key technology of semiconductor fabrication, the definition of lateral structures.

One of the fundamentals of our society is the storage and handling of information. The need for quicker processing of more and more data is the driving force for the development of microelectronic devices. In 2000 the critical dimensions of most important microelectronic devices, the Metal Oxide Semiconductor Field Effect Transistors (MOSFET), which are the heart of almost every integrated circuit, are about 180 nm; in 2001 this measure will be scaled down to 130 nm. The International Technology Roadmap for Semiconductors [2], which identifies the technological challenges and needs facing the semiconductor industry over the next 15 years, indicates a further shrinkage of this dimension down to 45 nm in the year 2013. This rapid development requires a huge amount of research and the advancement of new technologies.

A brief insight will be given here into the ongoing methods of lithography and the physical limitations. In Sec. 1 a survey is given, in Sec. 2 so-called optical lithography and its progress are discussed in detail. In Sec. 3 extreme ultra violet lithography and in Sec. 4 x-ray lithography are discussed. Another promising candidate for sub-100 nm patterning is lithography with electrons, which is described in Sec. 5, while lithography with ions is addressed in Sec. 6. Sec. 7 deals with the matter of resists and in Sec. 8 an insight in the issue of the alignment of several mask layers is given. As an example of non-lithographic patterning, "nano-imprint Lithography" is introduced in Sec. 9.

The term "lithography" describes the method with which a pattern is defined on a sample. A lithographic system consists of a radiation source, a resist-coated sample and an image control system that regulates which part of the sample is illuminated by the radiation and which is not (Figure 1a). The resist is changed by the illumination (Figure 1b). Depending on the type of resist, the exposed (positive tone process) or the unexposed resist (negative tone process) can be removed selectively by a developing process (Figure 1c). The pattern is now inscribed into the resist and can be transferred to the sample by a subsequent process step, e.g. an etching step. The name *resist* stems from this step, which is not actually part of the lithography process: The resist is resistant to the etching agent, so that the parts of the sample which are still covered by the resist are protected against etching.

Figure 2 shows a survey of the different types of lithography. They differ according to the type of radiation and the control system. However, the starting point of the process is the structure, which has to be transferred to the sample; it is normally given as a

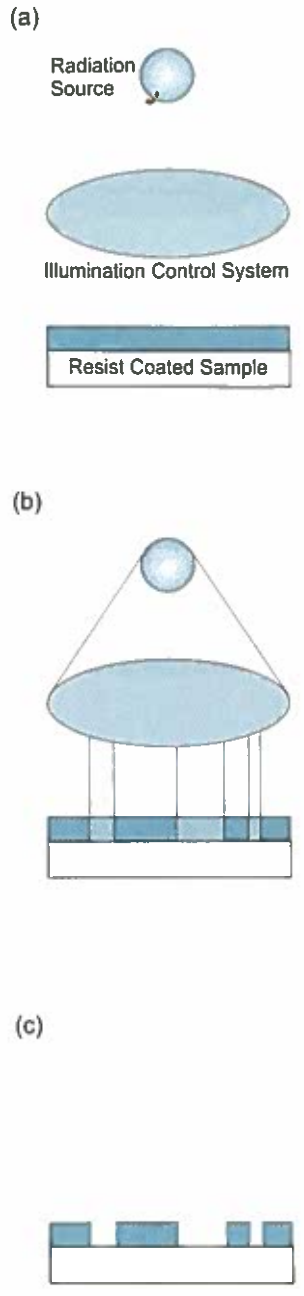

Figure 1: Schematic process flow of lithography with a positive tone resist: (a) A lithographic system consists of a radiation source, an illumination control system and a resist-coated sample; (b) Illumination Process: The resist is changed by the radiation, (c) Development: The illuminated resist can be etched selectively to the unexposed resist.

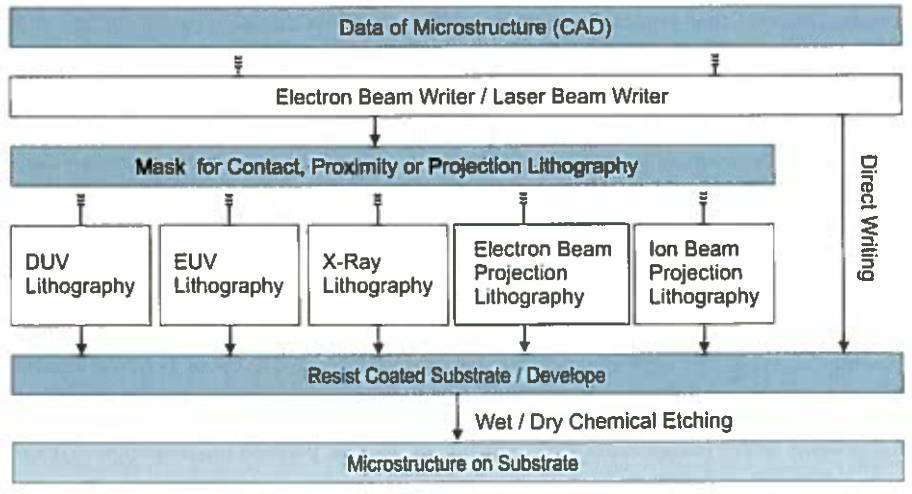

Figure 2: Survey of the different types of lithography.

CAD-file. The use of light as radiation yields so-called *optical lithography*. Depending on the wavelength, a distinction is made between ultraviolet (UV: 365 nm – 436 nm), deep UV (DUV: 157 nm – 250 nm), extreme UV (EUV: 11 nm – 14 nm) and x-ray (< 10 nm). The use of electrons or ions as radiation yields electron or ion lithography, respectively.

As the image control system either a *mask* is used, which yields *contact*, *proximity* or *projection lithography*, or the patterns are directly written into the resist by a focused beam (*laser*, *electron* or *ion beam lithography*).

With the first method, the mask consists of a carrier material, which is transparent for the radiation used, and an absorber layer, which is opaque. Into this opaque layer, the pattern is inscribed. The material depends on the radiation source and is addressed later. The radiation will only illuminate those parts of the sample where the corresponding part of the mask is transparent. Therefore only at those parts the resist is exposed and hence changed.

With *direct writing* a computer controls a focused beam of the used radiation. With deflecting units, the beam is scanned across the sample so that the pattern is written into the resist as if using a pen. Here every pattern has to be written after the other so that it takes a long time to finish a whole wafer. The development process is the same as for mask-based lithography. The relevancy of direct writing lies in its research purpose and in mask fabrication. There the mask itself is the resist-coated sample.

2 Optical Lithography

Optical lithography is the most important type of lithography. Originally the name referred to lithography using light with wavelength in the visible range. Nevertheless, gradually, the wavelength was driven down to 193 nm, which is used in semiconductor production nowadays, and even shorter wavelengths down to the sub-nm rage are under investigation.

The key issue of lithography is the resolution of the system, and hence the size of the smallest feature (minimum feature size: *MFS*) which can be defined on the sample. This *MFS* depends on the illumination method, the illumination wavelength λ, on the materials of the optical system and the resist used. In Sec. 2.1 the different illumination methods and their physical resolution limits are addressed, in Sec. 2.2 the wavelengths and the light sources are discussed, also for wavelengths below 15 nm, while lithography with these wavelengths is discussed in Sec. 3 and 4, and in Sec. 2.3 the materials and the forms of the optical system are dealt with.

2.1 Illumination Methods and Resolution Limits

Figure 3 shows a schematic view of the three different illumination methods *contact*, *proximity* and *projection lithography*. With all three, the light emitted by a light source passes a condenser optics so that a parallel beam is formed. With contact lithography, mask and sample are pressed together so that the mask is in close contact to the resist (Figure 3a). The resolution is limited by deflection and is expressed by the *MFS* which can be obtained. For contact lithography this is: $MFS = \sqrt{d \cdot \lambda}$, where d is the resist thickness and λ the wavelength. For a resist thickness of 1 µm and a wavelength of about 400 nm, this yields a minimum feature size of 600 nm. The major drawback of this method is that the quality of the mask suffers from contact to the resist, leading to failures in the structure. To avoid this problem, the second method was developed (Figure 3b). With *proximity lithography* there is a defined proximity gap g between sample and mask, so there is no deterioration of the mask. The drawback is the poorer resolution limit, which is proportional to $\sqrt{(d+g)\cdot\lambda}$. With same figures as above and a proximity gap of 10 µm, the *MFS* is 2 µm.

The method used today in industrial production is so-called *projection lithography* (Figure 3c). Here not the shadow of the mask is transferred to the sample as with the two other methods, but a picture of the mask is projected onto the sample. Therefore after passing the mask, the light is bundled by an optical system. The mask is not in contact with the sample, so there is no deterioration as in contact lithography, but the resolution is better than in proximity lithography. Furthermore it is possible to reduce the picture so the patterns on the mask are allowed to be bigger than the patterns on the sample. This is

advantageous for mask fabrication: Errors are also reduced. If it is possible to obtain masks with an accuracy of 100 nm, then the error for a structure of 500 nm to be transferred onto a sample is 20 %, if it is transferred one by one. If the picture is reduced 4 times, then for a 500 nm feature on the sample, the feature on the mask has to be 2 µm; therefore the mask error is only 5 %. Because of the reduction, the wafer is not exposed in one exposure, but in several . This is done by so-called steppers, in which the wafer is adjusted under the mask by an x-y-table. The stepper moves the wafer from one exposure position to the next, while the mask is not moved.

In projection lithography the limiting factor to the MFS is diffraction. Consider a slit width b which is illuminated by a monochromatic plane wave. What will the intensity distribution look like on a screen at a distance l behind the slit? Therefore consider two Huygens waves, one from the lower rim of the slit, one from the middle. There will be an optical path difference between these two Huygens waves, depending on the angle of propagation Θ. The magnitude of the path difference (*PD*) is:

$$PD = \frac{b}{2}\sin(\Theta) \tag{1}$$

The two Huygens waves will interfere destructively if the *PD* is an odd multiple of the half wavelength:

$$\frac{b}{2}\sin(\Theta_{min}) = (2m+1)\cdot\frac{\lambda}{2} \qquad \text{with } m = 0, \pm 1, \pm 2, \ldots \tag{2}$$

Under this condition, the Huygens waves from the lower part of the slit will interfere destructively with the ones from the upper part. At the angle Θ_{min} there is a minimum of intensity.

The Huygens waves do interfere constructively resulting in a maximum of intensity when:

$$\frac{b}{2}\sin(\Theta_{max}) = m\lambda \qquad \text{with } m = 0, \pm 1, \pm 2, \ldots \text{ holds.} \tag{3}$$

In lithography the diffraction patterns of several structures are superimposed so the question leading to the MFS is the question of when two structures can be resolved. The first approach is given by the Rayleigh criterion [3]. When light coming from a point source passes an optical system a blurred diffraction pattern – the Airy disc – occurs. The Rayleigh criterion says that two ideal point sources (e.g. stars) can be resolved when the intensity maximum of the one Airy disc is in the first minimum of the other, so *MFS* is given as:

$$MFS = 0.61\cdot\frac{\lambda}{NA} \tag{4}$$

where *NA* is the numerical aperture of the optical system. Nevertheless the Rayleigh criterion is just a first approach to the *MFS* in microlithography. The mask patterns are not independent (i.e. incoherent) ideal point sources, on the contrary they have a finite width and the light is partially coherent. Nevertheless, the form of the criterion gives the right dependences. If the wavelength is decreased by 10 % or the *NA* is increased by 10 %, the *MFS* is improved by 10 %. Furthermore, it was derived only by properties of the optics although the photoresist also affects the MFS. Therefore more generally, the criterion is written as:

$$MFS = k_1\cdot\frac{\lambda}{NA} \tag{5}$$

where k_1 is a constant (typically 0.5 – 0.9), which accounts for non-ideal behaviour of the equipment (e.g. lens errors) and the influences which do not come from the optics (resist, resist processing, shape of the imaged structures,...). Therefore k_1 is called the technology constant.

As a comparison, for a technology constant of 0.7 and a numerical aperture of 0.7, which are commonly used figures, the *MFS* is in the order of the wavelength λ. So it is better by about a factor of 0.66 than the *MFS* of contact printing.

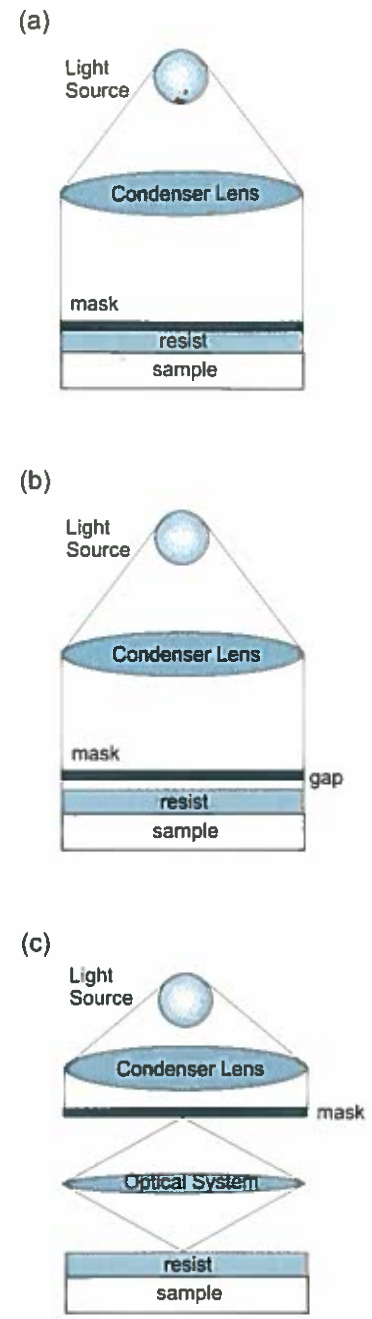

Figure 3: Lithography methods:
(a) contact,
(b) proximity and
(c) projection lithography.

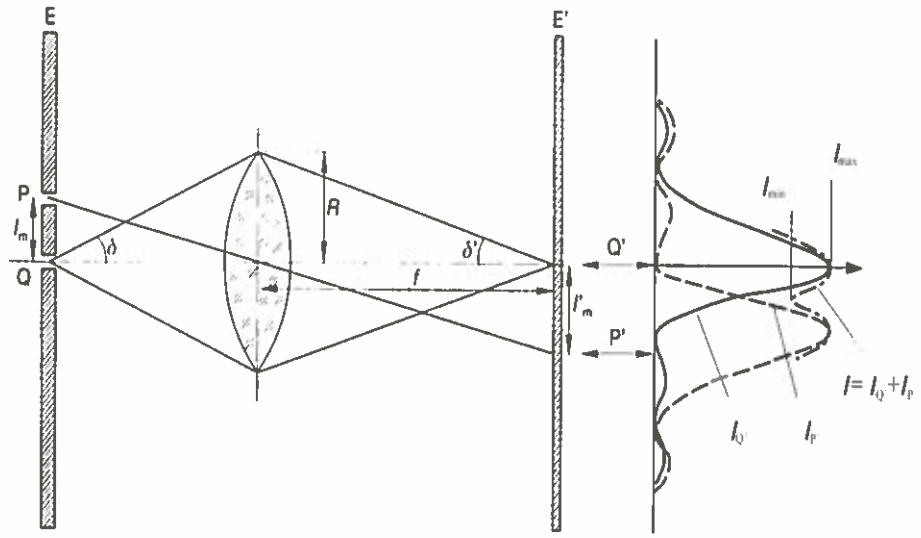

Figure 4: Intensity pattern of two features *P* and *Q* at projection lithography. The intensity distribution at the sample is broadened due to deflection [4].

Figure 4 clarifies the connection between mask, diffraction and intensity distribution in the image plane. Due to diffraction two sharp features, P and Q, on the mask give rise to an overall intensity distribution on the sample. To resolve these two features the intensity distribution has to have a minimum between the two main maximums. It is useful to define the so called modulation transfer function (*MTF*) as:

$$MTF = \frac{I_{max} - I_{min}}{I_{max} + I_{min}} \qquad (6)$$

The higher the value – the higher the difference between the maximum and minimum intensity – the better the contrast between exposed and unexposed areas, the better is the resolution of the equipment. It should be noted that the *MTF* is only derived by properties of the optical system. It is a measure of the capabilities of the lithographic tool in printing structures.

Resolution Enhancement

For a given tool and technology, the resolution is a given figure. There have been several attempts to improve this essential figure without any major changes to the tool (i.e. no other wavelength or *NA*). Figure 5 shows the possible places where changes can be made in the optical path to improve resolution. Two of these attempts are discussed in the next subsections, the phase shift techniques and off-axis illumination. In off-axis illumination, the effective light source is tailored, while in phase shifting techniques the wave edge of the illuminating light is tailored by the mask.

Phase Shifting Techniques

A huge improvement in resolution and/or in depth of focus can be obtained by improving the contrast by tailoring the phase differences of the wavefront. The phase difference is changed by varying the optical path length of the light passing through the vicinal structures, leading to constructive and destructive interference, which improves contrast (i.e. increase I_{max} or decrease I_{min}). To understand the method the approach proposed by Levenson in 1982 [26] is discussed.

Consider a lines and spaces structure with pitch $2p$. Figure 6 shows at the left hand side the amplitudes and intensities in the case of a conventional mask. At the mask itself, the normalized amplitudes are of rectangular shape (either +1 or 0) and give a proper image, but the light is diffracted into the dark regions and so the amplitude distribution is broadened as shown in Figure 6. The intensity of the light is the square of the sum of the amplitudes, so there is an intensity distribution with a significant I_{min} between the maximum intensities.

Now consider the case when the amplitudes of the light passing through the vicinal structures are out of phase by π (i.e. +1, 0 and –1) (Figure 6, right hand side). Again the light is diffracted into the dark areas, but now the light interferes destructively: There is a point where the sum of the amplitudes is zero, so the intensity is zero, too. These

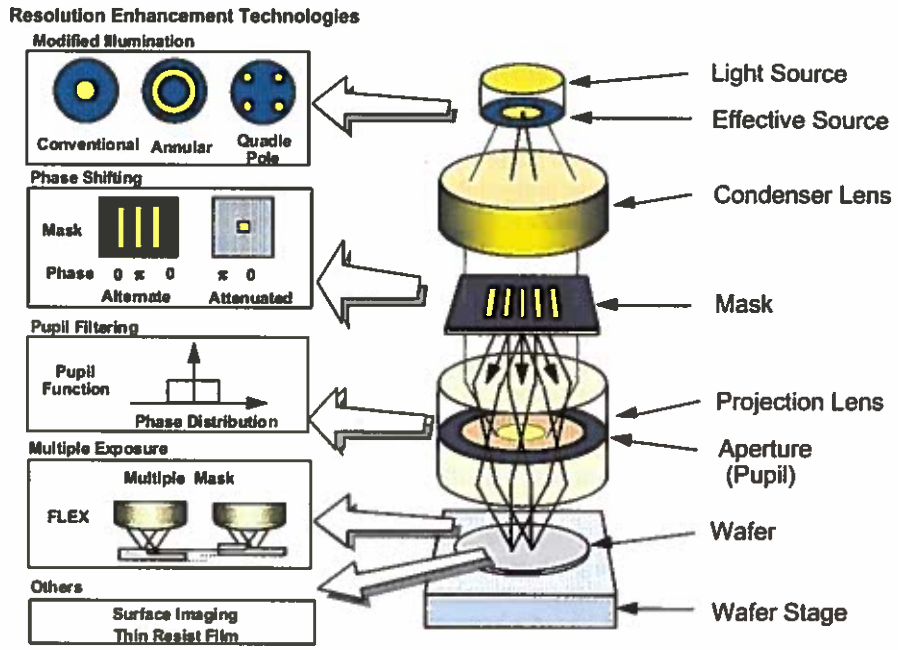

Figure 5: Survey of the resolution enhancement techniques.

so-called *Levenson* or *alternating phase shift masks* (PSM) can improve the resolution by 40 %. Unfortunately, this improvement is pattern-dependent; for a single structure there is no neighboring structure, so there is no light to interfere with. Even if there are structures which are not in a regular arrangement, there is no defined phase shift between these structures which could yield an improvement in the resolution of all structures.

The phase shift can be obtained by an additional transparent layer on the mask. If it has the refractive index n and thickness d, the phase shift is $\Phi = (n-1)2\pi d/\lambda$. So a shift of π is obtained, when the condition $d = \lambda/[2(n-1)]$ holds. On the other hand, it is also possible to recess the mask material so that the right optical path difference is obtained. But the etch depth can be controlled by the time only, and not, as in etching away an additional layer, by the thickness of the layer itself.

To deal with the drawbacks of alternating PSM, several other methods have been developed, which are described next. In rim-PSM, the whole mask is covered by a phase-shifter material and then with the resist. After development, the phase shifter is etched anisotropically and the masking layer is etched isotropically. By this a undercut under the phase shifter occurs at the rim of every structure. This also yields a resolution improvement, but not as much as with alternating PSM, although it is therefore not limited to certain structures.

Another way to engineer the optical path lengths is attenuated PSM. Here the opaque layer is replaced by a partially transparent (about 10 %) layer. The light passing these semi-opaque areas is not strong enough to expose the resist, by it can interfere with the light passing the transparent areas. So an improvement of resolution can be

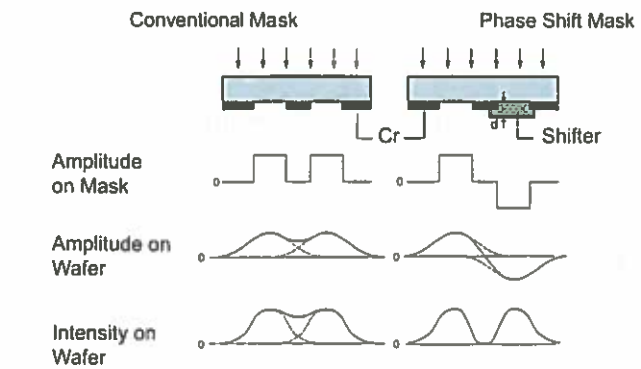

Figure 6: Comparison of the light amplitudes and intensities at the mask and on the wafer for a conventional and a phase shift mask. Note that the intensity on the wafer between the two features is zero for the phase shift mask [26].

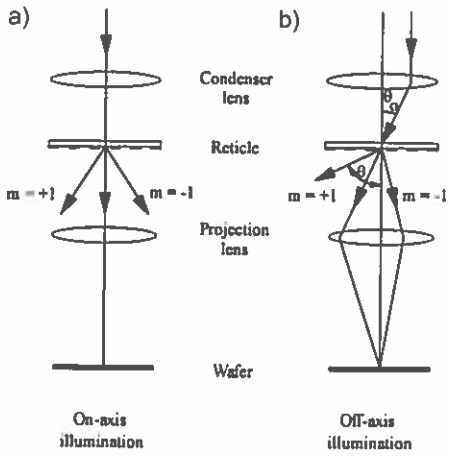

Figure 7:
(a) Optical path and deflection orders of on-axis and
(b) off-axis illumination. Note that with the same wavelength and structure size, the off-axis illumination allows the 1st order beam to pass the optical system [3]. A good description of off-axis illumination is also found in [6].

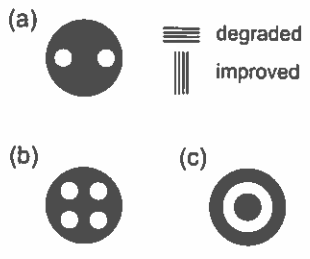

Figure 8: Apertures facilitating off-axis illumination.
(a) improvement of resolution perpendicular to the holes in the aperture,
(b) improvement in up-down and left-right direction, but not in diagonal direction and
(c) improvement in all directions [3].

obtained. The advantage of attenuated PSM is the easier mask processing. There is no extra layer as in alternating or rim PSM. The technology to process the semi-transparent layer is in principle the same as with a *normal* opaque layer.

PSM techniques were introduced in 1982, but only from 1999 they have been used for industrial production. An example which illustrates the impact of PSM methods is the results published by INTEL on the International Electron Device Meeting (IEDM) in 2000. A 248 nm phase-shiftmask lithography tool was used to produce a MOSFET with a 30 nm gate length [36].

Off-Axis Illumination

To improve resolution without decreasing the wavelength or increasing *NA*, so-called off-axis illumination was applied. The method was already known as a contrast-enhancing technique for optical microscopes. With off-axis illumination, the light beam is directed from the mask towards the edge of the projection lens, and not, as in on-axis illumination, towards the center. In normal illumination with partially coherent light, there always is part of the light which is off-axis, but in the context here with off-axis illumination there is no on-axis component.

To understand the mode of operation of off-axis illumination, consider a line-and-spaces structure with pitch p. The incident light will be diffracted into a set of beams, of which only the undiffracted beam, the zero-order beam, travels in the direction of the incident light. The 1st order beam travels under the angle $|\theta_1| = \arcsin(\lambda / p)$. If p is too small, then $|\theta_{\pm 1}|$ is bigger than the acceptance angle α of the projection optics, then only the zero-order beam is projected to the sample (Figure 7a). But this does not carry any information of the pattern, and hence the pattern cannot be transferred onto the sample. At least the zero- and the 1st order beam have to be in the range of the aperture angle. If the incident light hits the mask under an angle $\Theta_0 < \alpha$ the undiffracted beam enters the projection lens at the edge, and the 1st order beam is still collected by the lens, and therefore a pattern transfer is still possible. The angle of incidence Θ_0 can be realized by inserting an aperture in the optical path between condenser and mask (Figure 7b).

Although the higher resolution is an advantage of off-axis illumination, the impact on the depth of focus (DOF) is of even greater value. In on-axis illumination, the beams of different deflection orders have to travel in different ways so they are phase-shifted to each other, which results in a lack of focus. In off-axis illumination, the zero order and 1st order beam reaches the projection lens at the same distance from the center, which means that their optical path length is the same. So the relative phase difference between these beams is zero, which increases the DOF dramatically.

Off-axis illumination is facilitated by an aperture (Figure 8) which is located in front of the condenser lens. It depends on the apertures shape which structures are improved. If there is an aperture as in Figure 8a, only the structures perpendicular to the arrangement of the apertures will be improved. The aperture shown in Figure 8b yields an improvement of structures which are adjusted to *good* angles – up/down or left/right direction. This is sufficient because in normal cases, the features are in a *good* arrangement. The aperture in Figure 8c even decreases this problem, but here the improvement in DOF is less.

When the resolution in principle has to be improved, then according to the Rayleigh criterion either the wavelength λ or the technology parameter k_1 have to be decreased, or the numerical aperture *NA* has to be increased.

Increasing *NA* means physically bigger lenses. Here the problem arises that it is difficult to produce huge lenses with the required quality; on the other hand the available materials also limit the physical size of the lenses. So there are still two possibilities of increasing the resolution: smaller λ and smaller k_1.

2.2 Exposure Wavelength and Light Sources

Progress in optical lithography in the last few years was achieved by decreasing the exposure wavelength λ from 436 nm to 193 nm nowadays; research is in progress to push this boundary down to a few nm. In this section the different wavelengths, the methods of obtaining that light and the implications for the process are discussed. In Tab. 1 the wavelengths, the sources and the names of the wavelength ranges are given.

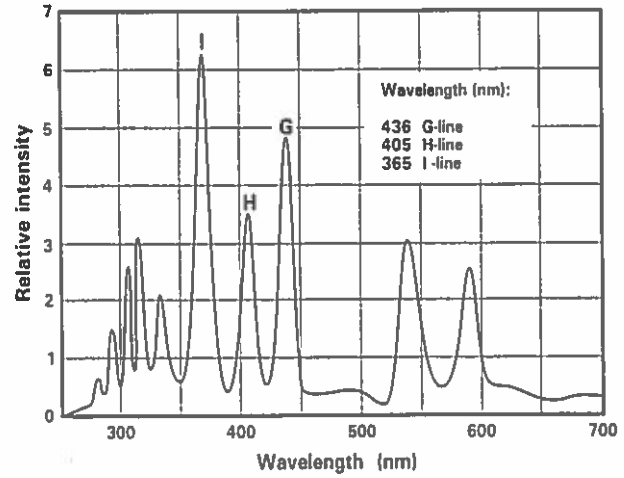

Figure 9: Spectrum of a high pressure Hg-lamp [46].

The first light used was the light emitted from Hg-arc lamps. It provides three lines, the G-line (436 nm), the H-line (405 nm) and the I-line (365 nm). A spectrum of a high-pressure Hg-lamp is shown in Figure 9. With typical k_1 and *NA* resolutions of ~400 nm were achieved. A further decrease of λ to 250 nm was obtained by a mixture of Hg and Xe, improving resolution to 300 nm, but the intensity at this wavelength is low.

To solve the intensity problem, at 250 nm a new light source occurs: the excimer laser. The word stems from *exited* and *dimer* and describes a molecule which only exists in an exited state. The gas mixture in an excimer laser is either KrF, ArF or F_2, resulting in the so-called deep UV (DUV) wavelengths of 248 nm, 193 nm and the vacuum UV (VUV) wavelength 157 nm, respectively. The excimer molecule consists of a noble gas and a halogen atom; in the ground state they cannot react, but if one or both are in an excited state, an exotic molecule can be formed. These dimer molecules decay into the ground state of both constituents with the emission of DUV light. The spontaneous decay time is long (i.e. nano- to microseconds), so inversion can be achieved by pumping the laser gas electrically.

In production DUV lithography with a resolution of 180 nm is used, while the boundary in research is being pushed down even further [36].

Wavelength [nm]	Source	Range
436	Hg arc lamp	G-line
405	Hg arc lamp	H-line
365	Hg arc lamp	I-line
248	Hg/Xe arc lamp; KrF excimer laser	Deep UV (DUV)
193	ArF excimer laser	DUV
157	F_2 laser	Vacuum UV (VUV)
~10	Laser-produced plasma sources	Extreme UV (EUV)
~1	X-ray tube; synchrotron	X-ray

Table 1: Illumination wavelengths, light sources and light ranges

Between 157 nm and ~13 nm is a huge gap where no usable wavelength exists. This is because all materials absorb light of that wavelength, so no masks, lenses and mirrors can be made. Nevertheless, when wavelengths in the range of 13 nm are used, it is possible to set up an optical path to do projection lithography. This range is called extreme ultraviolet (EUV). Shrinking the wavelength into the range of 1 nm leads to x-ray lithography. Here it is not possible to perform projection lithography because there is no material to set up an optical system (see Sec. 4).

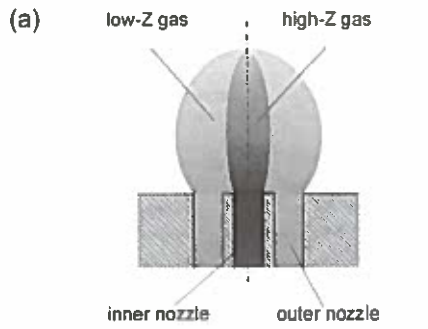

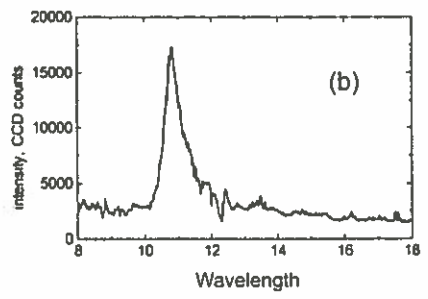

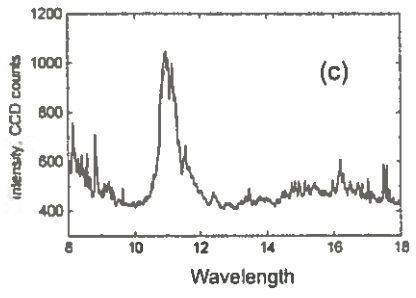

Figure 10:
(a) Double nozzle injector of a laser produced plasma source; through the inner nozzle the high-Z gas and through the outer nozzle the low-Z gas is injected, both gases form the target. Spectral distribution spectrum for the spectral image of
(b) a double stream Xe/He target and
(c) an ordinary Xe target [8].

The methods used to generate this light are the same for both ranges. All of them have to meet certain requirements such as being efficient enough at the desired wavelength and have low debris production (or feature a mechanism to avoid the contamination of tool and sample).

Firstly an x-ray tube can be used. In an x-ray tube, a metal anode is radiated with high energy electrons so that the characteristic x-ray radiation of the metal is emitted. The wavelength can be adjusted by the right choice of metal and electron energy. Unfortunately there are two drawbacks. On one hand, the intensity of these sources is very low leading to exposure times of several hours. This may match the requirements for research purposes, but surely not the ones of industrial production. On the other hand, the anode metal is sputtered and contaminates the exposure tool and the sample. This leads to unwanted loss of intensity, which decreases the lifetime of the tool and destroys the sample. In summary, x-ray tubes do not meet the requirements for EUV or x-ray lithography.

To a second group of methods the gas discharge sources belong. There are different types under investigation. While they differ in the concepts of plasma ignition, geometry of the source and discharge parameters, they all have in common that a plasma is generated by a fast discharge of electrical energy and emits thermal radiation in the EUV range. In common, gas discharge sources still suffer from debris. Nevertheless, in recent years some progress has been made with these issues [29], [30].

Another kind of sources is the laser-produced plasma sources (LPP). A pulsed laser focused on a target consisting of oxygen, fluorine, neon or xenon excites a plasma discharge in the desired wavelength region. The target is either solid (cryogenic), liquid or gaseous. The method is almost the same for all cases: The target is injected into a vacuum. Onto the jet a laser is focused, whereby the plasma is stimulated. The drawback is that the debris problem is not solved at all. For plasma excitation the gas has to have a certain pressure, therefore the distance between the plasma and the injector is too short so that the injector is sputtered. For liquid xenon targets [7] or a double gas target [8], which are under development, the debris problem is reduced. In a double gas target, the Xe-injector is surrounded by a second injector, from which a low-Z gas (He) is injected. The He encloses the Xe so that the distance between the injector and the plasma can be larger; therefore there is less debris and hence less contamination. Figure 10a shows a cross section of the injector, Figure 10b a space-integrated spectrum from a double-stream Xe/He target and Figure 10c the same for an ordinary Xe target.

The only light source which is luminous enough, at least in the 1 nm-wavelength range, and where no debris is produced is a synchrotron source. Electrons are accelerated onto a circular path and hence emit bremsstrahlung. But the synchrotron source is very expensive and therefore the cost of expanding lithography by one tool is very high. Also the shielding of the synchrotron is a drawback for these sources.

The question of which source will be used as an EUV or x-ray source is still not decided. While synchrotrons meet the optical requirements for wavelengths in the 1 nm-range, they are very expensive both with respect to purchasing costs and the clean-room space they require. X-ray tubes are suitable only for research purposes, while LPP offers a sufficient light quality for development, but not for production. Discharge sources still suffer from debris, but they are cheaper to purchase cost of ownership. Good comparisons between the different sources are given in [31], [32].

2.3 Mask Materials and Optical System

2.3.1 Set-up of the Optical Path

It is possible to obtain light with wavelengths from <1 nm to 500 nm. But besides the light source supplying light of a certain wavelength, an optical system has to be set up to do lithography. Masks, mirrors and lenses are needed which are suitable for the used wavelength. This is expensive.

There are two concepts for setting up the optical system. On the one hand, it can be designed with refractive elements (e.g. lenses: refraction optics). In a refraction optics system, the light passes the mask and lenses. Therefore these components have to be made of transparent materials. But the transmission through the materials depends on the wavelength. While soda-lime glasses and borosilicate glasses were used in earlier IC fabrication, these glasses become too less transparent as the wavelength approaches 250 nm. Furthermore, these materials have a high thermal expansion coefficient ($\approx 93\times10^{-7}\,K^{-1}$), which leads to a significant expansion of the masks when it is heated by the absorbed light. Fused silica, used instead, is transparent enough for even 193 nm

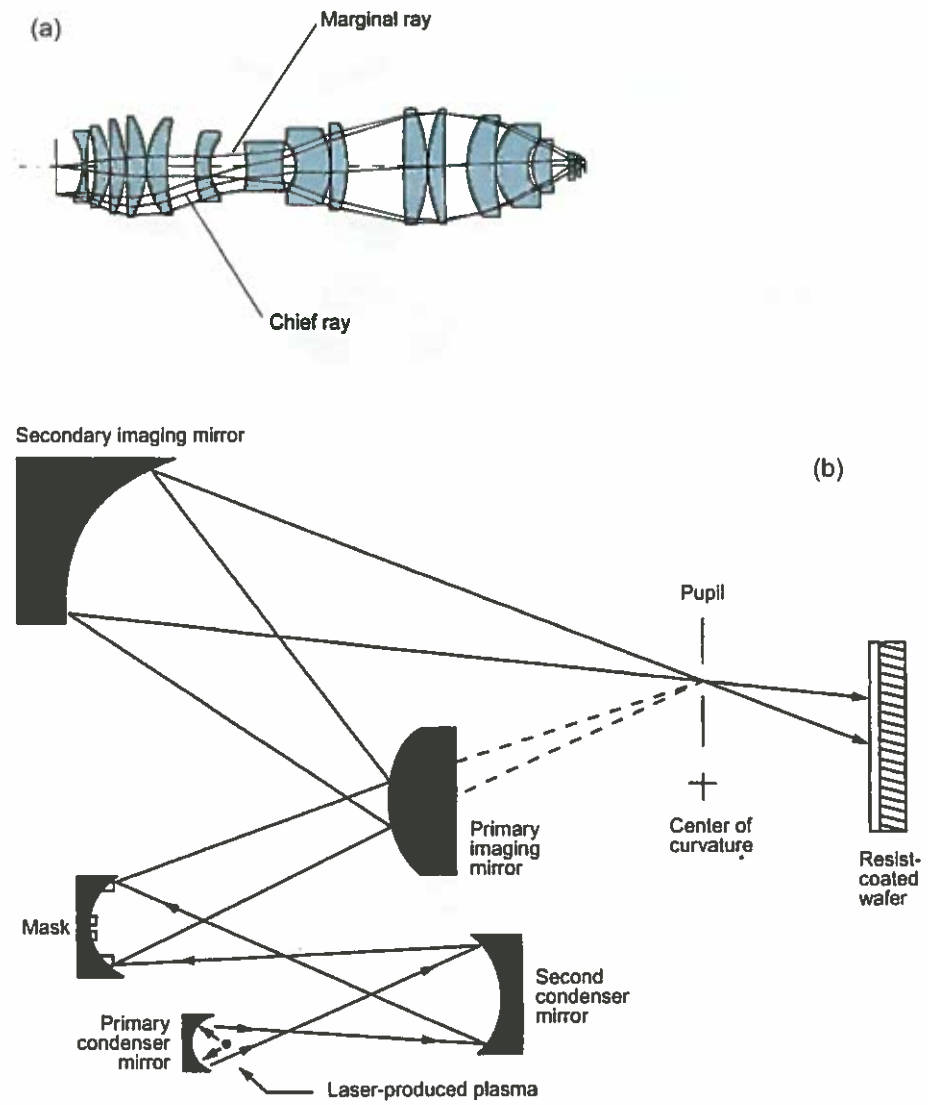

Figure 11: Setup of optical paths:
(a) refraction optics [3],
(b) reflection optics [37],
(c) catadioptric [41].

(Figure 12) and has a thermal expansion coefficient of about 1/20 of the other glasses. Nevertheless, even with the low coefficient of $5\times10^{-7}\,K^{-1}$ a temperature change of 0.1 K results in a displacement error of 5 nm, which is more than 10 % of the allowed tolerances for 0.25 µm technology. Below the 193 nm boundary other materials have to be used. One candidate under investigation is CaF_2 and its alloys [9]. These materials also have to fit another boundary condition: The defect density of the material has to be as low as possible in the mask as well as in the lenses to avoid projection errors. Due to the high *NA* of the optics, this is a rather strong condition.

On the other hand, an optical path can be designed for the use of mirrors (reflection optics). With reflection optics, the light is bundled by a concave mirror, and even the mask is a mirror, whose reflectivity is spatially altered according to the desired structure. Regions with high reflectivity correspond to exposed regions on the wafer, regions with low reflectivity correspond to the unexposed regions. In catadioptric systems some parts of the optical path are made up of reflection and some of refraction optics elements. The advantage of reflection optics is the higher spectral bandwidth, so achromatic lens error can be avoided. On the other hand, such a system normally requires more than one optical axis, therefore it is difficult to align the elements.

It is also possible to combine both parts (catadioptric system). The design depends strongly on the wavelength in use (Figure 11).

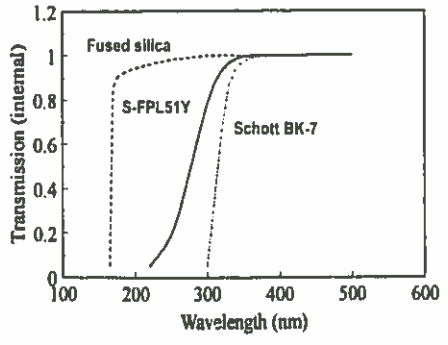

Figure 12: Transmission of different silica glasses. Below 170 nm normal quartz-based glasses become unsuitable for lithography [3], [42].

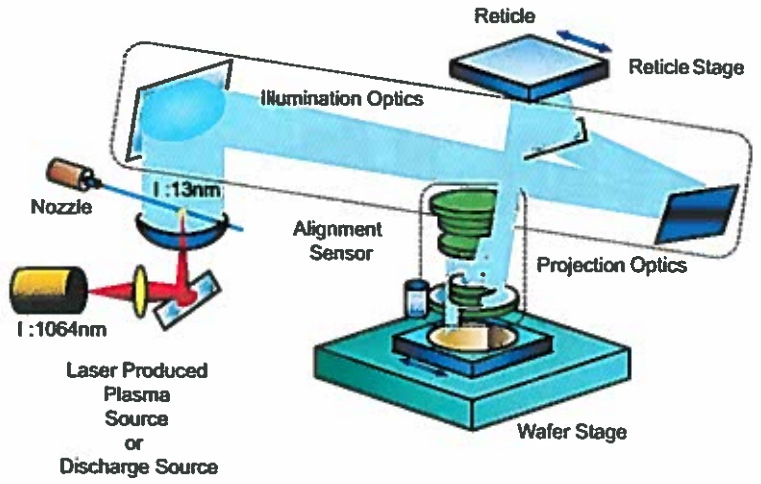

Figure 13: A schematic view of the EUV exposure system.

2.3.2 Reflection optics for short wavelengths

In the range from 10 to 15 nm (EUV) there is now material which is transparent enough to permit refraction optics, but there are no materials which can be used as a mirror. Therefore the mirrors are made up of a so-called *Bragg reflector*. Such a reflector is made of a layer stack, in which a high-refractive index material and a low-refractive index material are deposited onto each other in alternating order. The optical thickness of each layer is $\lambda/4$. At every interface some part of the incident beam will be transmitted and some part will be reflected. The transmitted beam travels to the next interface and again is transmitted or reflected. This second reflected beam will reach the first interface (again partly transmitted and reflected), and the now transmitted beam will interfere with the first reflected beam. The optical path difference is $\lambda/2$, but one of the reflected beams is reflected at an interface coming from a material with a higher refractive index and so there is a phase shift of π, i.e. $\lambda/2$. The whole path difference is therefore λ and the two beams interfere constructively. The optical path length is dependent on the angle of incidence, so the reflectivity also depends on that angle. This is the reason, why the optical path has to be designed for small angles of incidence as well.

3 Extreme Ultraviolet Lithography

EUV lithography is one of the promising candidates for next generation lithography (NGL). Efforts are being made in the USA (EUV-LLC/VNL) was formed in 1997 [33], in Japan there is an ASET program [34] and in Europe the EUCLIDES project has been implemented [35]. In EUV a wavelength of 13 – 14 nm is used. The resolution capability is determined by the Rayleigh criterion as in optical lithography. At such a short wavelength region, no refractive optics can be used, but only reflective mirror optics. Figure 13 shows the schematic view of the EUV exposure system.

As shown in the previous section, only a Bragg reflector (multilayer mirror) can be used in this wavelength region. For the 13 – 14 nm region, the mirrors are made of more than 40 repetitions of Mo/Si and show reflectivity of up to 70 %. Because of the low reflectivity (at least in comparison with optical mirrors) of these reflectors, the number

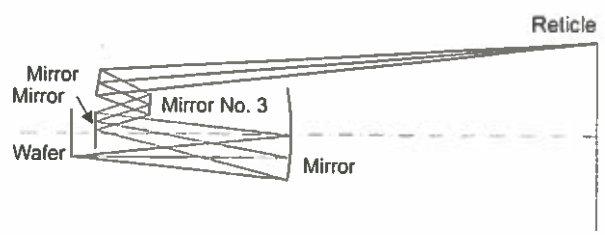

Figure 14: An example of the EUV 4 reflective mirror optical path.

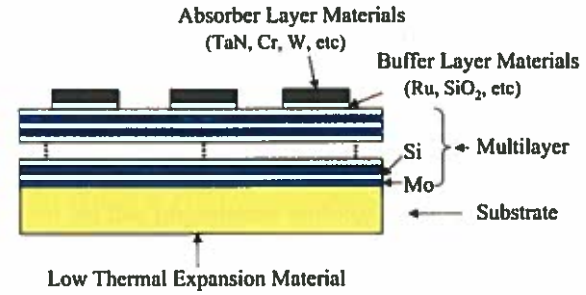

Figure 15: Schematic view of the multilayer mask.

of mirrors has to be kept small in the whole optical path. In the conventional projection optical lithography system, more than 25 lenses (namely more than 50 surfaces) are used for composing an aberration free projection optics. Almost all the surfaces of these lenses have a spherical shape. On the contrary, in the optics of EUV lithography system only 4 – 6 aspherical mirrors are used. The reason for the use of aspherical surfaces is to impose various aberration correction functions onto one mirror surface. Figure 14 shows an example of an EUV 4-mirror reflective mirror optical path. The biggest issue of the aspherical mirrors is the accuracy of the aspherical surface. Three major errors are minimized for the mirror: namely the figure errors, the mid-spatial frequency roughness and the surface roughness . Each error must be less than 0.20 nm, 0.15 nm, and 0.10 nm in rms respectively. The metrology of the figure error is very challenging, various visible and exposure metrology systems are being intensively developed.

In the case of reflection optics, the numerical aperture of the system cannot be so high as that of refraction optics because the incident light reflected by the mirror goes to the same direction as that from which the light ray comes. To avoid interference between the incident light and the reflected light, the usable solid angle is restricted. The maximum *NA* of the optics is 0.3 or smaller. However, even though such a small numerical aperture is used , as the exposure wavelength is very short, such as 13 – 14 nm, the resolution capability is expected to be very high. Currently it is thought that EUV lithography can be applied to 35 nm technologies and below.

The EUV mask must also be a reflective mirror mask. Figure 15 shows the schematic view of the mask structure. The very low thermal expansion material is used for the substrate. Mo-Si multilayer is deposited on the substrate and absorber patterns are made on the multilayer [12]. As an absorber layer, a material which shows very high EUV light absorption material should be adopted. Heavy metals are therefore good candidate materials. However, as the absorber patterns should be inspected by DUV light, DUV contrast should also be considered. Currently, Cr and TaN are thought to be good candidates. To delineate absorber materials, a buffer layer must be inserted between the absorber layer and multilayer to avoid damage to the multilayer during absorber patterning. For this purpose, SiO_2 and Ru are under investigation.

Defect reduction in the deposition process of the multilayer is one of the most critical issues in the multilayer mask process. The ion beam sputtering method is widely adopted for this purpose because the defect generation during the ion beam sputtering is lower than that of magnetron sputtering. However, the reflectivity of the multilayer deposited by the ion beam sputtering system is usually slightly lower than that deposited by the magnetron sputtering system. In the case of the multilayer of the optical mirror, as the reflectivity is more important than defect density the magnetron sputtering system is widely used.

Defect detection is a very important issue for the evaluation of the multilayer mask. A very small (2 – 3 nm in height) bump in the multilayer introduces a phase defect. A special defect inspection system is required for the inspection of the multilayer mask.

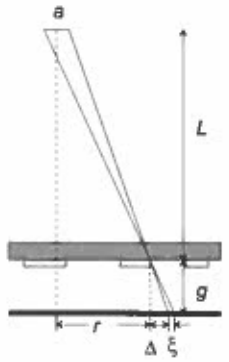

Figure 16: Penumbral blur ξ and displacement error Δ for proximity x-ray lithography. L is the distance from source to mask, g is the proximity gap and a is the lateral diameter of the source [11].

4 X-Ray Lithography

Decreasing the wavelength even further into the x-ray range yields so-called x-ray lithography. For these short wavelengths it is not possible to set up an optical path neither in reflection optics nor in refraction optics. On one hand, there is no material which is transparent enough to make lenses or masks from, and, on the other hand, it is not possible to make Bragg-reflectors. The individual layers in the layer stack have to have a thickness of $\lambda/4$, which corresponds to a layer thickness of ~0.3 nm. This is in the range of the thickness of one monolayer and is not achievable..

Projection x-ray-lithography is therefore not possible, but proximity x-ray lithography (PXL) is possible. The advantages are the high resolution limit ($\sim\sqrt{\lambda\cdot(g+d)}$), which is about 30 nm for 1 nm exposure wavelength) and the insensitivity to organic contamination. These contaminations (as all low atomic number materials) do not absorb the x-rays, and hence are not printed onto the sample.

But there are some limitations. Consider a source with diameter a of 1 mm at distance L of 1 m towards the mask and a proximity gap g of 10 µm. Then there is the so-called *penumbral blur* $\xi = a\cdot g/L \sim 10\,\text{nm}$, which limits the resolution (Figure 16). Furthermore, the pattern is not transferred correctly to the sample. Even if a point source is used, there is a displacement Δ of $\Delta = r\cdot g/L$, where r is the radial position on the sample (Figure 16). This error can be eliminated if it is taken into account when the mask pattern is generated.

Nevertheless, if synchrotron radiation is used, a high intense beam of parallel light is available so these errors do not occur. This parallel beam has another advantage: Due to the small deflection the exposure shows a high depth of focus of several µm, facilitating exposures of textured substrates or of thick resists (Figure 17).

The problem for PXL is the masks. Since there is no material which is as transparent to x-ray as quartz to DUV, the carrier layer has to be thin (1 – 2 µm). On the other hand, there is also no material which is as opaque to x-ray as chromium to DUV, so the masking layer has to be thick enough (300 – 500 nm). A carrier layer of 1 µm SiC only has a transparency of 57 %, while a masking layer of Au still lets 14 % of the light pass. The absorbed light will heat the mask so that it expands, which leads to another uncertainty in the pattern transfer. Furthermore, PXL is a non-reduction printing method, so the features on the mask are of the same size as on the sample. This makes the production of the masks very complicated when the target ist the sub-100 nm range.

The mask production sequence is as follows: On a silicon wafer, a thin membrane layer is deposited (e.g. SiC, Si_3N_4). Onto this layer, a chromium etch stop layer and the masking layer of 300 – 500 nm of a high-atomic number material is evaporated (e.g. Au, Ta). Then the mask is coated with an e-beam resist and exposed in an e-beam direct-write system. The resist is used to etch the masking layer with an etch stop on the chromium so the membrane is not hurt.

The commonly used DUV resists show good process aptitude.

5 Electron Beam Lithography

Another way to achieve sub-100 nm resolution is to change the type of radiation. In the foregoing sections only lithography methods were discussed which use light as the illuminating radiation. It is also possible to achieve the illumination with charged particles such as electrons. Electrons can be easily generated, either by thermionic or field effect emission, and focused to beams with a spot size of a few nanometers. This electron beam can be used to write the desired structure directly into the resist (Sec. 5.1) or using appropriate electron optics to perform electron projection lithography (Sec. 5.2). The chemical reactions in the resists are the same as in optical resists, only the reactive species has to be tuned to the electrons (nevertheless some optical resists can be used as electron beam resists, too).

5.1 Electron Beam Direct Write

In electron beam direct write electrons are formed to a beam and are accelerated to a determined position on the wafer surface, where the resist has to be exposed to form the pattern. An electron beam system consists of the electron source or electron gun, the electron-optical system (the electron column), a mechanical wafer stage and a controller system. A schematic view of an electron beam lithography tool is given in Figure 18.

The two types of electron guns which are commonly used are thermionic sources, on the one hand, and field emission sources, on the other hand. In thermionic sources the electrons are emitted by heating the source material, such as tungsten (W) or lantanum hexaboride (LaB_6). While LaB_6 offers a higher brightness (10^5(A/cm^2)/steradian)) and a longer lifetime (~1000 h) than W (10^4(A/cm^2)/steradian; ~100 h), W has the advantage that vacuum requirements are not as high as for LaB_6. Nevertheless, LaB_6 has become the standard source for thermionic e-beam sources.

In field emission sources the electrons are extracted from a sharp tip by a high electric field. Though these sources have a high brightness (10^7(A/cm^2)/steradian)), they are unstable and require a ultrahigh vacuum. Therefore they have not been widely adopted in electron beam lithography systems.

In the electron column the extracted electrons are formed to a beam with a definite diameter or shape. Therefore different electron-optical elements as focusing and defocusing lenses and apertures are employed. Further parts of the column are a beam blank to switch the beam on and off and a beam deflection system, with which the beam is positioned on the wafer.

Since the deflection system can only address a field of 400 – 800 µm (depending on spot size and tool), it is necessary to move the sample under the beam from one exposure field to the next by a mechanical wafer stage. The position of the stage is measured by an interferometer, so it is possible to adjust the beam with an accuracy of ~5 nm.

The whole system has to be under vacuum to enable the electron beam to be formed and has to be isolated from vibrations. Further requirements are low electromagnetic stray field, because this would hamper the positioning of the beam.

The pattern, which is given as a CAD file, is translated into movements of the electron beam/wafer stage by a computer. During an illumination, the tilt of the sample is measured continuously and the focus is adjusted. There are two exposure schemes: In the first one, the raster scan scheme, the deflection system and the wafer stage address every point of the sample, but the beam is switched on and off according to the structure. In the second scheme, the vector scan scheme, only the points which have to be illuminated are addressed. Hence the vector scan scheme is less time-consuming than the raster scan scheme.

The time needed for the illumination of a whole wafer depends on the pattern, but because the electron beam direct write is a serial method, it is time-consuming and not suitable for the industrial mass production of microelectronic circuits. Nevertheless, because the resolution is pushed to a few nanometers, it has a high impact on research activities and is the method of choice for defining the pattern on the masks used for optical lithography.

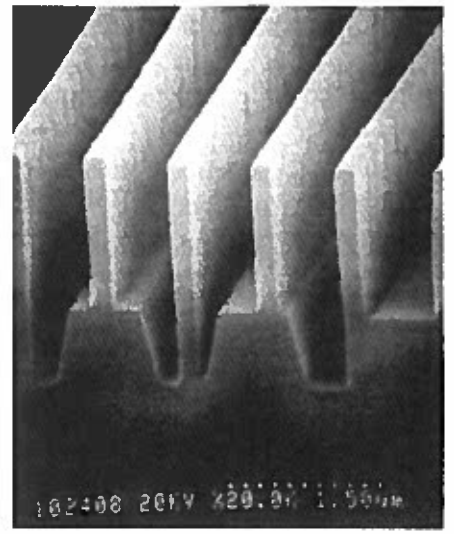

Figure 17: Resist structures on sample with high topography visualizing the high depth of focus of x-ray proximity lithography [10].

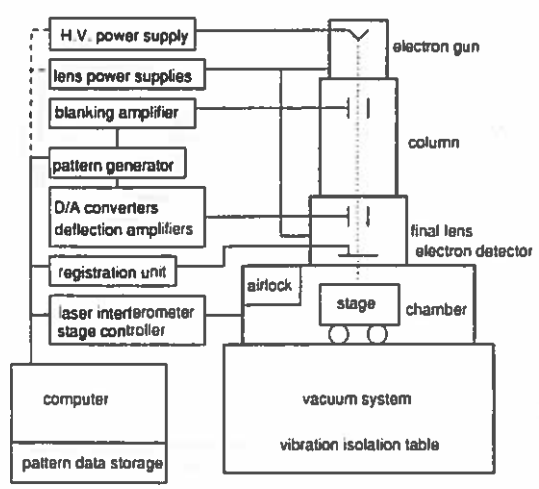

Figure 18: Schematic view of an electron beam lithography tool [16].

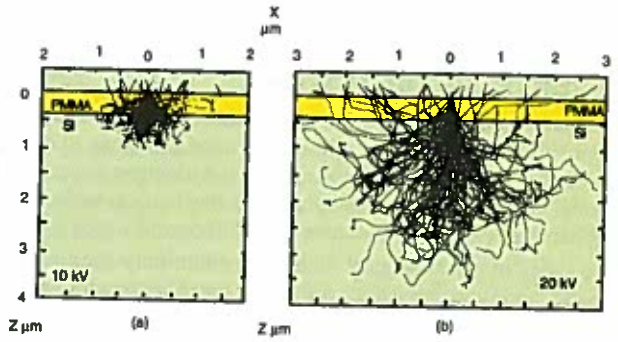

Figure 19: Monte Carlo simulations of the electron path in the resist and in silicon for 10 kV (left hand side) and 20 kV (right hand side) acceleration voltage. It is seen that there is a significant intensity of backscattered electrons in the vicinity of the written pattern [45].

The resolution is not limited by the deflection of the 1–100 keV electrons, but by the beam spot size (~5 nm achievable) and by the backscattering of electrons. Figure 19 shows Monte Carlo simulations of the electron paths, which have an energy of a) 10 keV and b) 20 keV. The electrons lose their energy slowly and a significant fraction of them are backscattered to the surface, where they expose the resist even at positions a few microns apart from the location of incidence. This so-called proximity effect leads to the fact that the effective exposure dose, with which the resist is exposed at one location, depends on the shape of the pattern in the vicinity and has to be taken into account when the pattern are developed (*proximity correction*).

5.2 SCALPEL

The drawback of electron beam direct write is the serial character of the method. In mass production, where throughput is concerned, exposure times of several hours are not acceptable. Though there are electron optics which could enable projection lithography analogously to optical projection lithography, this method suffers from the huge penetration depth of electrons. The masking layers have to be thick to stop a significant part of the electrons.

One method of circumventing this problem is the SCALPEL method (scattering with angular limitation in projection electron beam lithography). In SCALPEL a broad beam of electrons, 2 to 3 mm in diameter, is scanned across a mask consisting of a silicon-nitride membrane layer (~100 – 150 nm), on which a patterned scattering layer (25 to 50 nm of gold or tungsten) is situated (Figure 20a). The electrons, which only strike the membrane layer, will pass this layer mostly unscattered, while the electrons, which strike the scattering layer, will be distracted strongly from their path. The unscattered electrons are focused through an aperture and projected onto the wafer, while the scattered electrons will be blocked. So a high contrast image can be achieved.

As a projection lithography method, SCALPEL offers the advantage of image reduction thus making mask fabrication easier. The mask itself consists of silicon struts, between which the membrane layer is clamped (Figure 20b). The width of the membrane corresponds to the diameter of the electron beam, while it is a few cm in length. By means of the projection optics behind the aperture the electrons coming from two different membrane areas separated by a silicon strut can be stitched together at the wafer, so circuits of 2 cm times 3 cm can be exposed.

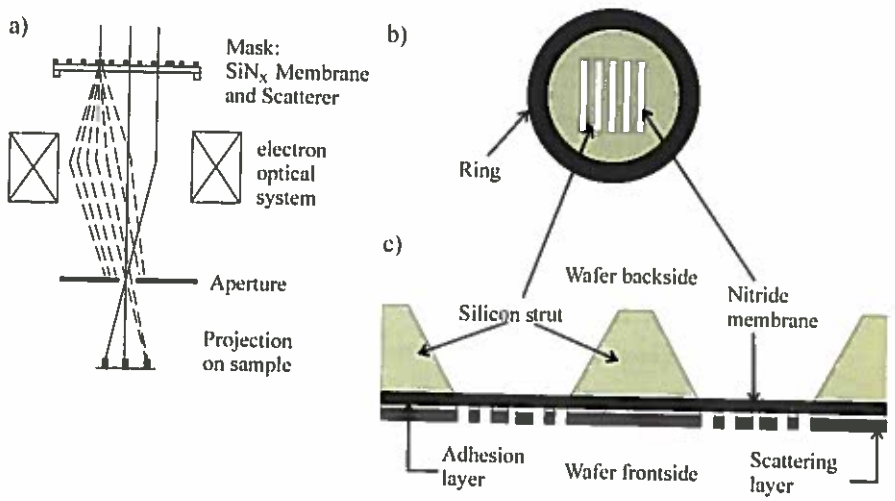

Figure 20:
(a) Electron path through a SCALPEL tool. A parallel beam of electrons passes through the mask; a scattering layer in which the pattern is inscribed scatters the electrons, so that they are not focused through an aperture by the electron optical system; only the unscattered electrons will pass the aperture. These electrons are projected onto the sample [16], [43].
(b) Top view of a mask and
(c) cross-sectional view of the mask. The masks are strips and separated by silicon struts. The masks are illuminated in series and the pictures of the masks are projected onto the adjacent sample .

There are still other approaches to Electron Projection Lithography, from which the PREVAIL (Projection Reduction Exposure with Variable Axis Immersion Lenses) method has to be mentioned. In PREVAIL the optical axis of the electron system is shifted, so aberrations are reduced, enabling larger scan fields. Theory and experimental data show, that PREVAIL can be able to meet the requirements for the 70 nm and 50 nm technology nodes [13], [14].

SCALPEL is able to resolve structures in the sub-100 nm region. Like other e-beam lithography tools, the limiting fact is not the wavelength of the electrons, but the proximity effect due to the significant backscattering of electrons. To circumvent these problems, heavier particles, e.g. ions, should be used. Ions will dissipate their energy much quicker than electrons and are stopped within the very vicinity of the location of incidence. Therefore there is no proximity effect.

6 Ion Beam Lithography

As electrons, ions can be used as radiation for lithography, too. As with electrons, a focused ion beam (FIB) can be used as the *pen*, or a broad beam can be modulated by a mask and than projected onto the surface (ion projection lithography).

6.1 Focused Ion Beam

The setup of a focused ion beam (FIB) tool is similar to an electron beam lithography tool, but instead of an electron beam a focused ion beam is used either to expose a resist locally, as in electron beam lithography, or to modify the substrate directly. The heavy ions impinging on the surface will sputter the material or, depending on energy, will intermix the layers at the surface of the sample. By means of this so-called ion milling the properties of the material at the surface will be altered. Another possibility is the local deposition of an additional layer. The impinging ions can induce the decomposition of a gas. As in a Chemical Vapor Deposition (CVD) process, where the decomposition of the process gasses is induced globally by thermal activation (Low Pressure CVD) or by a plasma (Plasma Enhanced CVD), this local decomposition leads to a local deposition of the material.

Besides a certain impact on the structure definition in the research environment, the direct modification of the surface, the sputtering as well as the deposition, enables the method to be used in the most important application of FIB in industry, namely mask repair. Mask production is very expensive and due to some failure in the processing (e.g. dirt sticking on the mask or a mistake in the electron beam pattern generator) a mask can be faulty. Either some parts of the masking layer, which should have been removed, are still present, or some parts of the masking layer are removed in excess. These faults can be cured by FIB.

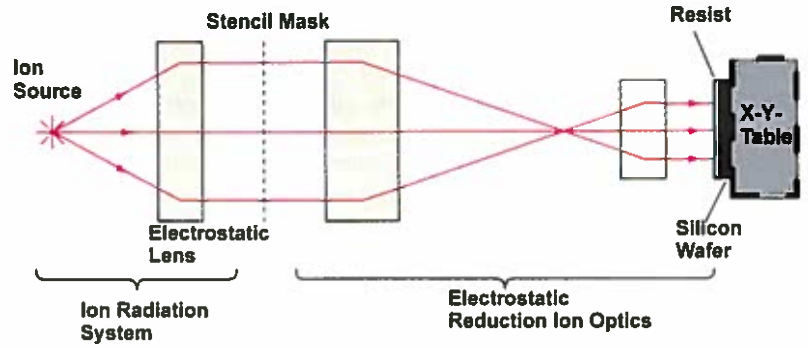

Figure 21: Schematic view of an ion projection lithography tool.

6.2 Ion Projection Lithography

Recently, ion projection lithography (IPL) has also been attracting increasing attention. Figure 21 shows a schematic view of an IPL tool. It consists of an ion source, electrostatic condenser optics, the mask carrier, projection optics and the wafer mount. The ions are emitted by an ion source and a parallel beam is formed by the condenser optics. This parallel beam of ions then illuminates the mask. Because of the low penetration depth of ions, the transparent part of the mask has to be made of nothing; even the thinnest membrane would stop the ions. The opaque parts consists out of a silicon wafer, which is protected against ion sputtering by a protection layer. This whole mask is called a stencil mask.

The mask technology for IPL is elaborate. The masks were fabricated from a silicon-on-insulator (SOI) wafer (a silicon wafer which has a buried oxide layer under a surface silicon layer). The patterns are inscribed on the top silicon. Then the bulk silicon and the oxide are etched. Only the patterned top silicon remains, serving as the absorber. Onto that layer the ion beam protective layer (carbon) is deposited, which hampers sputtering of the mask by the ions themselves.

Because of the stencil structure, it is not possible to define every structure in one run, e.g. it is not possible to write a circle: The middle will fall off. Therefore two masks with corresponding layout have to be used for one lithographic step. Furthermore the

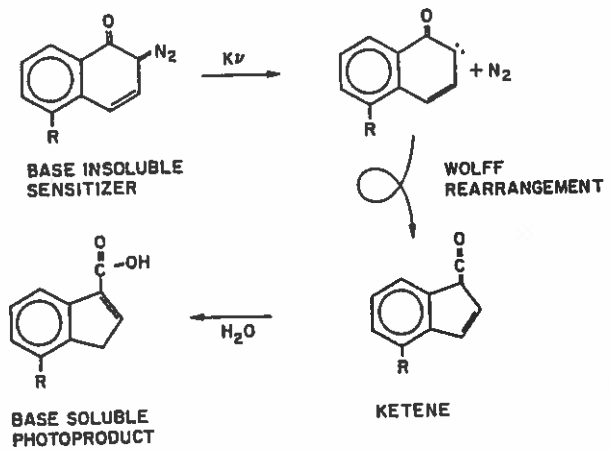

Figure 22: Exposure process of positive tone DNQ-resists [38], [39].

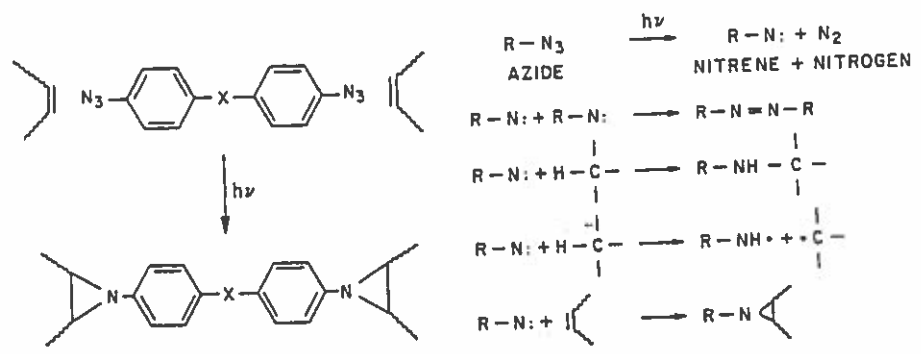

Figure 23: Reaction cycle of a negative tone resist during exposure [38], [39].

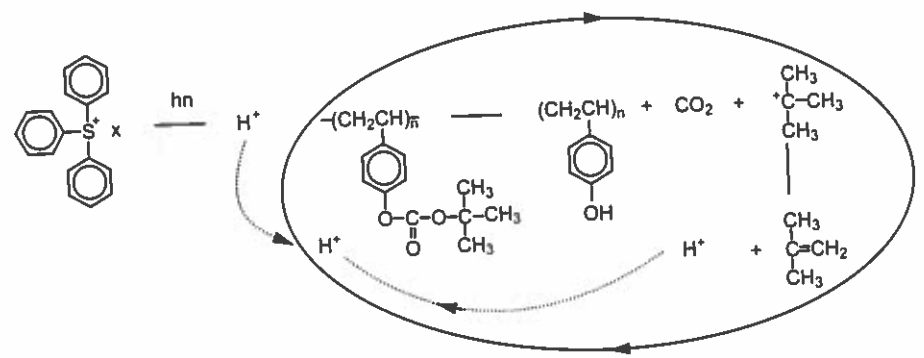

Figure 24: Chemical amplification cycle in a CAR [40].

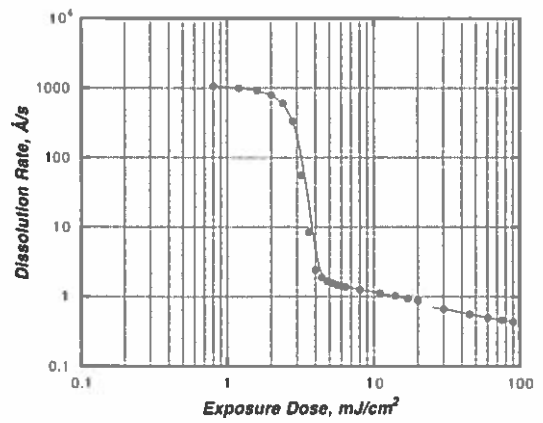

Figure 25: Contrast curve of the Shipley UVN30 DUV negative tone resist. The contrast curve shows the development rate of the resist versus the exposure dose. The steepness of the transition is high for a high contrast resist [44].

effect of gravity has to be taken into account. The distortion of the mask is dependent on the pattern itself, and so the splitting of the pattern into different masks is also a highly sophisticated problem. A good survey article is given in [17].

The IPL-tools are able to resolve 75 nm [27], but technical improvements can push this boundary down further. As an example of direct modification of the surface, the development of magnetic hard discs is given. Here a multilayer of Pt and Co is exposed by the projected ion beam. Using heavy ions, the layers will intermix and change their magnetic behavior, so the magnetic domains are formed [28].

7 Photoresist

Photoresists are also an integral part of lithography. The performance of the resist is the determining factor for the magnitude of the technology factor k_1. In general, photoresists are polymers which react when exposed to light. There are two different types of resists: With positive tone resists, the exposed areas of the resist will dissolve in the developer, with negative tone resists, the exposed areas will remain.

Positive tone resists consist of three components, a resin, which serves as a binder and establishes the mechanical properties, a photoactive compound (PAC), and a solvent to keep the resist liquid. The resin is not normally responsive to the exposure. The commonly used positive tone resist system for g- and i-line lithography is the novolac/diazonaphthoquinones (DNQ) system. The novolac is the resin material and dissolves in aqueous bases. The DNQ is the PAC, but when unexposed it acts as a dissolution inhibitor. Figure 22 shows the reaction cycle of the DNQ upon exposure. Upon exposure N_2 is split off the molecule. After a rearrangement, the molecule undergoes a reaction with the H_2O, which stems from the air. The reaction product now does not behave as a dissolution inhibitor, but as a dissolution enhancer. Therefore the exposed areas of the resist will dissolve about 100 times quicker than the unexposed areas.

Negative tone resists also consist of the three compounds: resin, photoactive compound and a solvent to keep the resist liquid. The resin consists of a cyclic synthetic rubber, which is not radiation-sensitive, but strongly soluble in the developer (non-polar organic solvents). The PAC is normally a bis-arylazide. Figure 23 shows the chemical structure of a rubber resin and a PAC. Upon exposure, the PAC dissociates into *nitrene* and N_2. These nitrene molecules are able to react with the rubber molecules, so a cross-linking between two rubber molecules can be established. Thus a three-dimesional cross-linked molecular network is formed, which is insoluble in the developer .

As device dimensions are scaled down further, the g-line steppers as well as the novolac/DNQ resists have been improved, so the features for 350 nm generation could be printed. But reaching the 250 nm generation, the illumination wavelength was shifted to 250 nm, too. However, at this wavelength novolac and DNQ do strongly absorb the light, therefore another class of resists had to be developed. Furthermore, the intensity of

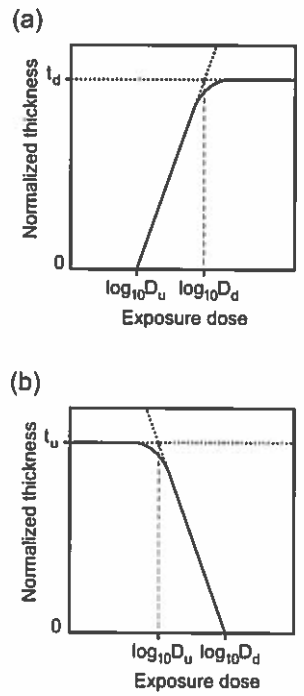

Figure 26: Schematic view of a contrast curve for (a) negative tone resist and (b) positive tone resist.

the mercury lamps at 250 nm was very low, so a high sensitivity of the resist was needed. The so called chemically amplified resists (CAR) use a chemical reaction to improve sensitivity and they are compatible with a 250 nm exposure wavelength. In a CAR, one of the compounds is a photo acid generator (PAG). Upon exposure an acid is released by PAG. During the post-exposure bake (PEB) – a heating of the sample after exposure – this acid reacts with the resin so that, firstly, the resin becomes soluble to a developer, and, secondly, a new acid is released. With this catalytic reaction it is possible to get 500 to 1000 reactions from one photogenerated molecule (Figure 24). Positive and negative tone CARs are available.

How do the resists affect the resolution? We have to consider the contrast of a resist: At what exposure dose is the resist exposed, and at what dose it is not yet exposed? As explained earlier, the light intensity at the sample is not of a rectangular shape, but is a diffraction pattern, so the resist at the sample is exposed according to that distribution. In Figure 25 a type of a contrast curve of a negative tone resist is given. In that curve, the etch rate of the resist in the developer is shown against the exposure dose. In an equivalent representation of the contrast curve, the normalized remaining resist thickness after a defined development process is plotted linearly against the logarithm of the exposure dose. For low exposure doses, the resist still behaves like an unexposed resist, for high doses it is fully activated. The transition between these two regions has to be steep to get a high contrast. To clarify this point refer to the intensity distribution of two patterns next to each other given in Fig. 4. The maximum intensity I_{max} has to be on the right side of the transition in Figure 25, the minimum intensity I_{min} on the left side.

The measure of the contrast is the contrast parameter γ. The higher γ the higher is the contrast, the closer I_{max} and I_{min} can be. It is determined as follows: The transition range of the contrast curve is fitted linearly the region where the resist is not etched by the developer (Figure 26a for negative tone resists, Figure 26b for positive tone resists). Where these two evens intersect, there is the dose D_u for positive and D_d for negative tone resists. The dose where the thickness of the resist becomes zero is D_d for positive and D_u for negative tone resists. The parameter γ is simply the negative slope of the contrast curve in the transition region on a logarithmic scale:

$$\gamma_{\pm} = -\frac{t_d - t_u}{\log_{10} D_d - \log_{10}(D_u)} = \frac{\pm 1}{\log_{10}\left(\frac{D_d}{D_u}\right)} \tag{7}$$

where t_d is the normalized thickness of the exposed resist, which means that t_d is 0 for positive tone resist and 1 for negative tone resist, and t_u is the normalized thickness for unexposed resist, so t_u is 1 for positive tone resist and 0 for negative tone resist; the sign stands for positive/negative tone resist, respectively. This characteristic can be expressed in terms of the so-called *critical resist modulation transfer function* $CMTF_{resist}$ which is defined as:

$$CMTF_{resist} = \frac{D_d - D_u}{D_d + D_u} = \frac{10^{\pm\frac{1}{\gamma}} - 1}{10^{\pm\frac{1}{\gamma}} + 1} \tag{8}$$

where the + stands for positive tone resist, and the – for negative tone resist. Now let us consider the exposure system with a given *MTF* with which a positive tone resist should be exposed. Choosing the exposure time s_e, with $I_{max} \cdot s_e = D_d$, $I_{min} \cdot s_e$ has to be less than D_u (otherwise I_{max} and I_{min} do not lie on the different sides of the slope of the contrast curve). Now :

$$MTF = \frac{I_{max} - I_{min}}{I_{max} + I_{min}} \cdot \frac{s_e}{s_e} = \frac{D_d - D_{min}}{D_d + D_{min}} \geq \frac{D_d - D_u}{D_d + D_u} = CMTF_{resist} \tag{9}$$

For a given *MTF* of the exposure system, the *CMTF* has to be smaller, and this means that the contrast of the resist has to be high enough.

Now let us consider the path of light in the resist. During exposure, the resist is not only traversed by the incoming beam, but due to reflection at the resist/sample interface, there are also reflected beams, giving rise to standing waves. The intensity variations emerging from these standing waves can be seen in the resist profile after development

(Figure 27a) and degrade the resolution. With CAR these ripples in the resist can be abolished by a thermal treatment after exposure (i.e. during a PEB). The reacted photoactive complexes diffuse, smoothening the side walls.

Furthermore, the exposure is not independent of the sample itself. Figure 27b shows simulated values of the linewidth transferred into the resist for two different samples – silicon wafers with oxide layers differing by the oxide thickness. It is seen that the linewidth depends strongly on the resist thickness and on the nature of the sample. This phenomenon stems from the reflections at the oxide/silicon interface and at the resist/oxide interface. To prevent these influences, anti-reflex coatings (ARC) are applied. It is possible to apply an ARC before the resist (bottom ARC) or afterwards (top ARC). With the BARC the reflectivity of the resist/substrate interface and with the TAR the reflectivity of the resist/air interface is minimized.

There are two possibilities to achieve this aim for BARC. First, the BARC could show a high absorption of the incident light. Unfortunately, if the absorption is high, the reflectivity of the BARC/resist interface will increase, degrading the effectiveness of the BARC. The second possibility is to match the BARC thickness and the refractive index, so that the optical path length of the BARC is $\lambda/4$. If the sample is exposed, the incident beam hits the resist/BARC interface, and is partially reflected and partially transmitted. The transmitted beam transverses the BARC, is reflected at the BARC/substrate interface and travels back to the BARC/resist interface. This beam and the first reflected beam are out of phase by $\pi/2$, so they interfere destructively, and the reflectivity at the BARC/resist interface is reduced. The TAR also has an optical path length of $\lambda/4$, so the interferences of the reflected beams are destructive.

BARC materials depend on the illumination wavelength and the samples. Spins on BARCs are primary absorption-type and consist of polymers. Oxinitrides deposited by PECVD can be used for index-matching type BARCs. The BARC layer has to be developed after lithography, requiring an additional process step. Figure 28a shows a resist structure without, Figure 28b with a BARC.

TAR can be spun on after spin coating. After exposure the TAR can be removed before development. Some TARs are designed to be developed in aqueous-based developer solution, which does not affect the resist. The handling of these TARs are much less complicated than the handling of BARC.

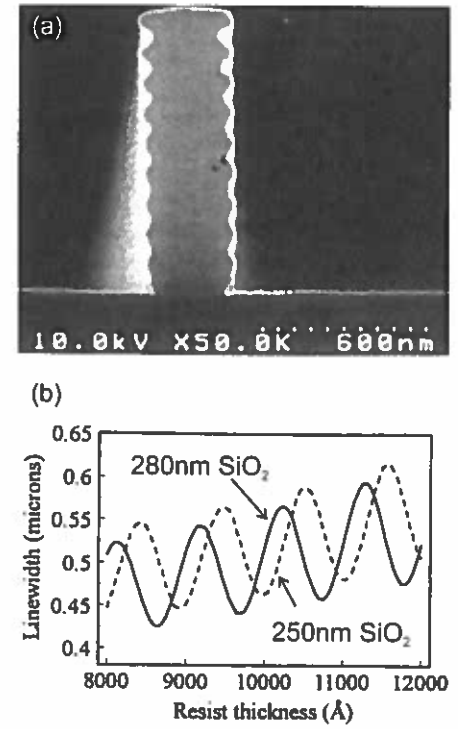

Figure 27:
(a) Impact of standing waves on the developed resist.
(b) Simulated linewidth as a function of resist thickness and substrate [3].

8 Alignment of Several Mask Layers

A modern microelectronic circuit needs several mask layers, which have to be properly aligned. For that purpose, every mask layer has so-called alignment marks: Special features on the mask whose positions are precisely known, and which are transferred to the sample by the subsequent etching or deposition step. The next mask layer also has an alignment mark at the corresponding position. Consider an exposure tool, in which the mask is loaded in a mask mounting fixture and the wafer on a movable wafer stage.

There are two systems of alignment in use. The off-axis alignment was developed first. The alignment marks on the sample were observed by a separate microscope using broadband non-actinic light as illumination to prevent the resist from being exposed. The wafer alignment marks were adjusted to marks etched into the microscope's objective. The mask was aligned independently to marks on the mask mounting fixture. This procedure would be enough for a single exposure if the mask and the wafer were separately aligned properly. But what is to be done if the wafer has to be exposed during several exposures as in a modern stepper? Admittedly, you know the structures to be transferred and you know the exposure positions on the wafer so it is possible to move the wafer stage to every exposure position, but the movement of the stage has to be very precise, and the long-term stability of the distance between alignment position and first exposure position, the so-called *base line* is difficult to achieve.

The second system is the through-the-lens alignment: Here, the image of the alignment mark on the sample is projected onto the corresponding mark on the mask and they are compared directly. One problem occurring with this system is the alignment illumination. A He-Ne-laser is used for this purpose so the resist will not be exposed, but the optics is not designed for that wavelength. Therefore the lens errors for that wavelength have to be corrected by additional lenses, which are brought into the optical path.

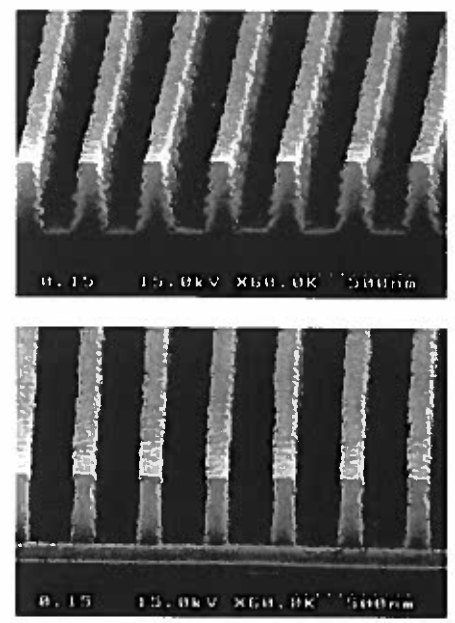

Figure 28:
(a) Resist structure without antireflex coating.
(b) Resist structure with ARC [15].

In contact and proximity lithography, the mask and wafer are aligned at every exposure. In modern projection lithography tools (e.g. a stepper), where the wafer is not exposed in one exposure, but in several exposures, attention has to paid for a accurate, quick and space efficient alignment. The wafer is moved by the wafer stage, while the mask is fixed. The position of the stage can be measured very precisely by three laser interferometers . Therefore some alignment strategies have been developed.

There are three degrees of freedom: x-shift, y-shift and rotation Θ. The first steppers used a technique called *two-point global exposure alignment*. In this strategy, one mark is used to adjust x- and y-shift, and the second mark is used to adjust Θ. Afterwards, the wafer is blindstepped through every exposure field. Here the movement of the stage has to be precise. To avoid this problem, a *zero-level alignment mark* can be used: this is a mark which is etched into the wafer before the process starts. Every mask-layer is aligned to that mark.

The next approach is the *site-by-site* alignment – that means performing the alignment at every exposure position. But this is time-consuming and, even a bigger drawback, there have to be alignment marks at every exposure position, which is a waste of space. Furthermore, the alignment marks on every site have to be small, so it is more difficult to detect them resulting in an increase in overlay error. So the *site-by-site* alignment strategy does not provide any advantage in comparison to a global mapping strategy as the 2-point-global-alignment strategy.

In the *enhanced global alignment strategy* 5 to 10 alignment marks are aligned and the stage position is measured several times. From the positions a least squares fit is computed. Based on these data, the positions of the exposure sites are corrected. These corrections are assumed to be stable for the time needed to expose the whole wafer.

The question of how to find the alignment marks and how to align them properly to each other is not discussed here, but the reader is referred to Ref. [47] and references therein for a survey of that topic.

9 Nanoimprint Lithography

There are several approaches for patterning structures without lithographic methods, e.g. a silicon surface can be modified by depassivation by the tunneling current in a UHV-STM (Ultra High Vacuum Scanning Tunneling Microscope [20], [21], or the surface can be modified by the movement of an Atomic Force Microscope (AFM)-tip . A certain interest has been focused on the nanoimprint lithography (NIL), which is described in more detail in this section.

With the NIL, a mold is processed by conventional technology, i.e. e-beam lithography and etching techniques, and is pressed onto a resist coated substrate. The structures in the mold are transferred into the resist and can be utilized after removing the mold. There are two different kinds of NIL, the hot embossing technique and a UV-based technique. A sketch of both techniques is given in Figure 29.

Hot Embossing Technique

Here the sample is heated above the glass transition temperature of the resist, which is a thermoplastic polymer. Above that temperature the polymer behaves as a vicous liquid and can flow under pressure. The mold itself can be made of different materials, usually a silicon wafer with a thick SiO_2 layer is used. This SiO_2 layer is patterned and structured by e-beam lithography and anisotropic reactive ion etching. The aspect ratio of the features are 3:1 to 6:1, and the mold size is several cm^2. As thermoplastic polymers either PMMA (a well known e-beam resist) or novolak resin-based resists are in use. PMMA has a small thermal expansion coefficient of $\sim 5\times10^{-5}\ K^{-1}$ and a small pressure shrinkage coefficient of $\sim 3.8\times10^{-7}\ psi^{-1}$. To ensure a proper removal of the mold, the resist is modified by release agents, which decrease the adhesion between mold and resist. Resist layers between 50 and 250 nm thickness are used. The imprint temperature and pressure are dependent on the resist. For PMMA the glass transition temperature is about 105°C, so the temperature at which the sample and the mold are heated is between 140 and 180°C. Then the mold is pressed onto the sample with pressures of about 40 – 130 bar. The temperature is then lowered below the glass transition temperature and the mold is removed. The features of the mold are now imprinted in the resist. The residual resist layer in these features is removed by anisotropic reactive ion etching.

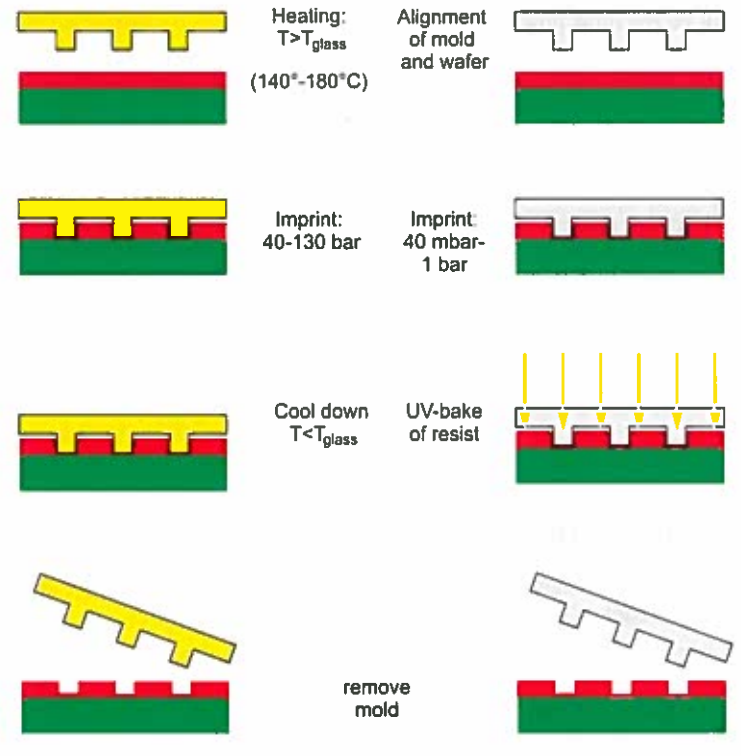

Figure 29: Nanoimprint lithography: hot embossing technique (left hand side) and UV nanoimprint (right hand side).

Afterwards, the structures can be transferred to the substrate either by direct etching or by metal deposition and lift-off. Structures down to a feature size of 10 nm for holes and 45 nm for mesas are imprinted with a high accuracy [22]–[24].

UV-based NIL

Heating and cooling of mold and sample is time-consuming. Therefore to achieve a somehow higher throughput, curing of the resist by UV irradiation is used. The thermoplastic resist is replaced by UV-curable monomers. The mold has to be fabricated of a UV-transparent material, e.g. quartz. The features are transferred to the mold by e-beam lithography and a Ti/PMMA resist stack. The patterned PMMA is used to transfer the features into the Ti, and the Ti is used to structure the quartz mold. The resists are acrylate- or epoxide-material systems, which can be modified with respect to low viscosity, UV curability, adhesion to the substrate and detachment from the mold. The low viscosity is essential for using low imprint pressures of 40 mbar – 1 bar. After pressing the mold on the sample, the sample is irradiated by UV-radiation through the mold and a baking, and hence a polymerization of the resist is initiated. This step lasts only about 90 seconds. After detaching the mold, the residual resist is removed by RIE and the further pattern transfer can be done. Again mold areas of several square centimeters can be imprinted in one run, and one imprint step takes about 10 minutes. The minimum feature size reported in the literature is 80 nm for dots. [25].

NIL offers the opportunity to define decananometer features in a rather *simple* manner, at least in comparison to the advanced lithography methods described above. The field size of $\sim 2\times2\ cm^2$ is comparable to a die which is illuminated by a stepper. On the other hand, this method is time-consuming (>10 min for one imprint) and up to now only structures on a plain surface have been investigated, while advanced lithography is able to define structures on textured substrates. Nevertheless, because of its technological simplicity, the NIL will be an alternative for research and small series production.

10 Conclusions

There are different approaches for achieving resolutions in the deep sub-100 nm region. EUV is being investigated by several projects (EUV-LLC in the USA, EUCLIDES in Europe and an ASET-program in Japan). But still the community is not sure about which method will be the most powerful. The SCALPEL method is being pushed forward by Lucent Technologies, and Infineon Technologies is involved with the development of IPL. All three methods are capable of resolving these fine dimensions, which have to be achieved within the next decade, but all three methods have their advantages and drawbacks. The EUV suffers from a very costly optics and mask technology, while for IPL and SCALPEL it is the small image area. The next five years will show which method will prevail.

For a deeper insight into the area of lithography there is a huge amount of good literature. Recommendable are [3], [10], [16], the Materials Research Society symposia, e.g. [18], and the annual conference Micro and Nano Engineering (MNE), from which e.g. [7] is taken . For theoretical purposes [19] gives a detailed description. For the whole environment of semiconductor technology refer to [11], for the future of semiconductors to [2].

Acknowledgements

The editor would like to thank Julio Rodriguez (FZ Jülich) for checking the symbols and formulas in this chapter.

References

[1] taken from *Chamber's Encyclopaedia*.

[2] International Technology Roadmap for Semiconductors (ITRS): http://public.itrs.net .

[3] H.J. Levinson and A. Arnold, in *Handbook of Microlithography, Micromachining and Microfabrication, Vol. 1,* SPIE, The International Society for Optical Engineering, Bellingham, WA, 1997.

[4] B. Hoppe, *Mikroelektronik,* Vogel, Würzburg, 1998.

[5] W. Waldo, in *Handbook of VLSI Microlithography,* Noyes Publications, Park Ridge, New Jersey, 1991.

[6] B. El-Kareh, *Fundamentals of Semiconductor Processing Technology,* Kluwer Academic Publishers, 1995.

[7] B.A.M. Hansson, L. Rymell, M. Berglund and H.M. Hertz, Microelectronic Engineering **53**, 667 (2000).

[8] H. Fiedorowicz et al., Optics Communications **184**, 161 (2000).

[9] E. Sarantopoulou, Z. Kollia and A.C. Cefalas, Microelectronic Engineering **53**, 105 (2000).

[10] F. Cerrina in *Handbook of Microlithography, Micromachining and Microfabrication, Vol. 1,* SPIE, The International Society for Optical Engineering, Bellingham, WA, 1997.

[11] C.Y. Chang and S.M. Sze, *ULSI Technology,* McGrawHill, 1996.

[12] D.G. Stearns, R.S. Rosen and P. Vernon, J. Vac. Sci. Technol. A**9**, 2662 (1991).

[13] H. C. Pfeiffer, Jap. J. Appl. Phys. **38**, 7022 (1999).

[14] K. Suzuki et al., Proc. SPIE **4343**, 80 (2001).

[15] S.H. Hwang, K.K. Lee and J.C. Jung, Polymer **41**, 6691 (2000).

[16] M.A. McCord, M.J. Rooks in *Handbook of Microlithography, Micromachining and Microfabrication, Vol. 1,* SPIE, The International Society for Optical Engineering, Bellingham, WA, 1997.

[17] R. Kaesmaier and H. Löschner, Microelectronic Engineering **53**, 37 (2000).

[18] MRS Symposium Proc. Vol. 584, *Materials Issues and Modeling for Device Nanofabrication,* MRS, Warrendale, PA, 2000.

[19] K.A. Valiev, *The Physics of Submicron Lithography,* Plenum Press, New York and London, 1992.

[20] J.W. Lyding, T.-C. Shen, J.S. Hubacek, J.R. Tucker, G.C. Abeln, Appl. Phys. Lett. **64**, 2010 (1994).

[21] J.W. Lyding et al., Appl. Surf. Sci. **130**, 221 (1998).

[22] S.Y. Chou, P.R. Krauss, P.J. Renstrom: Appl. Phys. Lett. **67**, 3114 (1995).

[23] S.Y. Chou, P.R. Krauss, P.J. Renstrom: J. Vac. Sci Technol. B **14**, 4129 (1996).

[24] S. Y. Chou, P.R. Krauss, W. Zhang, L. Guo, L. Zhuang: J. Vac. Sci. Technol B **15**, 2897 (1997).

[25] M. Bender, M. Otto, B. Hadam, B. Vratzov, B. Spangenberg, H. Kurz: Microelectronic Engineering **53**, 233 (2000).

[26] M. Levenson et al., IEEE Trans Electron Dev. ED-29, 1828 (1982).

[27] W.H. Bruenger, MRS Fall Meeting 2001. Symposium Y3.5.

[28] R. Berger et al., MRS Fall Meeting 2001, Symposium Y3.4.

[29] M.A. Klosner, W.T. Silvfast, Opt. Lett. **23**, 1609 (1998).

[30] K. Bergmann, O. Rosier, R. Lebert, W. Neff, R. Poprawe, Microelectronic Engineering **57**, 71 (2001).

[31] R. Lebert, et al., Microelectronic Engineering **57**, 87 (2001).

[32] V.Y. Banine, J.P.H. Benschop, H.G.C. Werij, Microelectronic Engineering **53**, 681 (2000).

[33] R.H. Stulen, Microelectronic Engineering **46**, 12 (1999).

[34] S. Okazaki, Proceedings SPIE **3676**, 238 (1999).

[35] J. Benschop, U. Dinger, D. Ockwell, SPIE **3997**, 34 (2000).

[36] R. Chau et al., International Electron Device Meeting, Technical Digest. IEDM (2000).

[37] A.M. Hawryluk, L.G. Seppola, J. Vac. Sci. Technol. B**6**, 2162 (1988).

[38] S. Wolf, R.N. Taubner, in *Silicon Processing for the VLSI Era*, Lattice Press, 2000.

[39] J. Bowden, in *Materials for Microlithography, Advances in Chemistry*, Series No. 266, American Chemical Society, Washinton D.C., 1984.

[40] R.D. Allen, W.E. Conley, R.R. Kunz, in *Handbook of Microlithography, Micromachining and Microfabrication,* Vol. 1, SPIE, The International Society for Optical Engineering, Bellingham, WA, 1997.

[41] US Patent ,4,953,960, *Optical reduction system*, David Williamson, inventor, filed July 1988 and granted Sept. 1990.

[42] Ohara i-line Glasses, Ohara cooperation, Kanagawa, Japan, Juni 1993; Schott Catalogue of Optical Glasses No. 10000 on Floppy Disc, Edition 10/92, Schott Glass Technology, Duryea, P.A.

[43] S.D. Berger et al., J. Vac. Sci. Technol. B**9**, 2996 (1991).

[44] Shipley DUVN30 product catalogue, Shipley Company, Marlborough, MA.

[45] D.F. Kayser, N.S. Viswanathan, J. Vac. Sci. Technol. **12**, 1305 (1975).

[46] HBO Mercury Short Arc Lamps for Microlithography *Technology and Application Guide* 2000/2001, OSRAM GmbH, Munich.

[47] A. Moel, E.E. Moon, R.D. Frankel, H.I. Smith, J Vac. Sci. Technol. B**11**, 2191 (1993).